On the Necessity of Three-Dimensional Considerations in Vehicular Network Simulation

Alexander Brummer*, Reinhard German* and Anatoli Djanatliev*
* Computer Networks and Communication Systems, Dept. of Computer Science, University of Erlangen-Nürnberg, Germany
{alexander.brummer,reinhard.german,anatoli.djanatliev}@fau.de

***Abstract*—Despite significant improvements concerning the level of realism in Vehicular Ad hoc Network (VANET) simulation, the effects of three-dimensional aspects are still neglected by the majority of packet-based simulation tools. In most of the cases, a planar projection of the road network in question is assumed, leading to a misrepresentation of scenarios including bridges, hilly terrain or elevated infrastructure. In this paper we show that the consideration of three-dimensionality in realistic scenarios can lead to significantly differing results compared to 2D-only simulations. We discuss the requirements and extensions which are necessary in order to provide a three-dimensional simulation environment. This includes the support for three-dimensional antenna patterns as well as a model covering environmental diffraction effects. We examine the implications of three-dimensional aspects on the results of a city-wide simulation scenario showing that the number of vehicles in reach decreases noticeably. The outcome of a second, more specific use case even indicates that proper functioning of this specific application might be completely compromised, in harsh contrast to the result of the common 2D simulation approach, emphasizing the importance of 3D VANET simulation.**

***Index Terms*—vehicular ad hoc networks, VANET simulation, three-dimensionality, antenna patterns, diffraction model**

I. Introduction

Car-to-x communication is an enabling technology that gains more and more importance in the context of current research trends such as connected mobility and autonomous driving. For the research and development of new protocols and applications based on Vehicular Ad-Hoc Networks (VANETs), simulations have become the preferred tool. Experimental field tests are a good way to test VANET applications in a realistic environment, however, such experiments are bound to the examined scenario and can hardly be scaled. On the other hand, theoretic models often struggle to deliver representative results due to the high level of abstraction. Therefore, the simulation of vehicular networks is widely utilized as it combines the advantages of the two approaches mentioned before [1].

The quality of simulation results in general strongly depends on the accuracy of the underlying models. Speaking of packet-based VANET simulation it can be noted that the degree of realism has increased constantly in the recent past. Various models have been developed representing different aspects which characterize car-to-x communications whilst trying to stay within the limits of computational costs. On the one hand, environmental factors influencing the signal on its way to the receiver have been examined. A popular example for this is the obstacle shadowing model introduced by Sommer et al. [2], taking into account the impact of buildings between sender and receiver. On the other hand, technology-related aspects have been covered, which led to detailed models properly representing the IEEE 802.11p [3] standard for example. Another major step forward was the bidirectional coupling of mobility and network simulation [4], which made it possible to cover the main idea of VANETs in the first place, i.e. influencing traffic by communicating with each other.

Nevertheless, most simulation frameworks seem to ignore another important aspect. They assume a two-dimensional environment only by simplifying the real-world scenario and projecting it to a planar road network. As a result, the communicating nodes as handled by the network simulation part all appear to be located in the same horizontal plane. The neglection of the individual altitudes of vehicles and obstacles causes many real-world scenarios to be represented insufficiently as the majority of investigated traffic environments are simply not perfectly flat. Due to the direct dependence of a VANET's topology on the position of the communicating vehicles, this simplification can lead to significantly differing results for the analysis of vehicular networks.

Examples for such problematic scenarios are not bound to a certain area, but can be found in urban, subarban and highway environments. A demonstrative three-dimensional road network is depicted in Figure 1. As can be seen, this highway interchange consists of multiple road layers stacked upon each other. Consequently, vehicles are located at varying altitudes. Antennas of communicating cars might have to

Figure 1. Sample 3D road network consisting of a complex highway interchange.

ISBN 978-3-903176-02-7

transmit or receive signals to or from near-vertical elevation angles. Moreover, the overpasses themselves will most likely lead to significant additional signal attenuation. A projection of this scenario to the horizontal plane would simply look like a complex intersection, disregarding all aforementioned considerations. Other examples of this kind may be found in environments with hilly terrain, simple overpasses, multi-storey parking garages or vehicles and infrastructure of different heights.

In this paper, we want to emphasize why three-dimensional considerations should not be neglected in VANET simulation and which essential extensions are necessary in order to achieve that. Therefore, we first summarize related work dealing with three-dimensionality in the context of vehicular networking. In Section III, we outline the necessary steps towards three-dimensional VANET simulation, including the generation of 3D road networks as well as extensions on the part of network simulation. Subsequently, we present two selected 3D scenarios that we simulated using the open-source framework Veins[1] extended accordingly. The results are finally discussed and compared to the outcome of the conventional simulation approach.

II. Related Work

Although not considered by most simulation frameworks, it becomes clear that 3D aspects and directivity characteristics do play a role in car-to-x communications when analyzing related research. A first example is the design of routing protocols for VANETs. Due to the fast-changing topologies position based routing protocols such as the Greedy Perimeter Stateless Routing (GPSR) [5] are very popular. The next hop is chosen with the objective to maximally decrease the distance to the destination node, which is why the position makes the difference in this type of forwarding strategy. In [6] Lin et al. investigate the applicability of GPSR in three-dimensional scenarios. They explain that usual position based routing mechanisms assume a two-dimensional vehicle distribution only, which can lead to suboptimal forwarding decisions. Using their novel Three-Dimensional Scenario Oriented Routing (TDR) protocol, the performance can be improved significantly by taking into account different road layers as well and preferring intra-layer transmission as far as possible. The authors finally compare TDR to GPSR based on a sample scenario featuring an overpass. With help of TDR the end-to-end delay in this specific scenario was decreased by 13 %, while the delivery ratio could be increased by about 40 %. These results indicate that the awareness of a 3D environment can be benefitial.

Not only implications on higher layer protocols have been identified, but also some effects on signal propagation. The obstacle shadowing model accounting for buildings along the line of sight (LOS) [2] has already been mentioned introductorily. However, also other vehicles between sender and receiver can cause noticable attenuation. Boban et al. showed that the LOS is often obstructed even by cars of similar heights and also under sparse traffic conditions [7]. Consequently, additional attenuation of up to 30 dB can lead to significant packet loss. In [8] the authors also come up with a potential solution to this issue. Using their Tall Vehicle Relaying (TVR) mechanism, taller vehicles such as trucks and vans are preferably selected for packet forwarding. Thanks to the elevated antennas there are less vehicles blocking the LOS so that transmission ranges increase by up to 50 %.

In the field of wireless communications another point strongly influences the signal. Antennas play an important role as they are the actual interface between device and wireless channel. They can show critically differing gains or losses depending on the direction. The resulting three-dimensional radiation patterns when mounting antennas on a car have been investigated in several papers [9], [10]. It could be shown that different antenna types and mounting positions on or under the car and on the side mirrors can lead to completely varying characteristics. Another interesting example is discussed in [11], where the mounting point behind a panorama glass window leads to severe attenuation towards the front. Despite such clear results antenna influence is hardly supported in VANET simulation. Just recently we have added the possibility of assigning two-dimensional antenna patterns to vehicles in Veins and showed that safety applications such as collision avoidance systems can be significantly impacted [12].

A method which already offers the possibility of investigating three-dimensional scenarios is ray tracing. Such simulations keep track of every signal's path and also consider reflections and scattering. Examples of this approach utilized in the context of vehicular communications are the aforementioned papers dealing with the implications of antenna patterns on the wireless channel [9], [10]. It is not surprising that ray tracing simulations are capable of producing highly detailed results. However, this maximum level of detail requires enormous computation performance and time. Moreover, every new scenario to be examined needs to be modeled in similarly high detail. Although there are already approaches to improve performance by making use of parallelized computations on GPU cores [13], ray tracing still involves considerable effort and is not suitable for large-scale scenarios. Thus, the consideration of 3D scenarios in packet-based VANET simulation would be very benefitial and will be discussed in the following sections.

III. Requirements for 3D VANET Simulation

In order to be able to simulate three-dimensional vehicular networks, the simulation framework in use has to be extended accordingly. While the presented approach was specifically implemented using the Veins framework, the outlined steps apply for any packet-based VANET simulator consisting of coupled traffic and network simulation. Therefore, there are necessary adjustments on both parts as well.

A. Generating 3D Road Networks

The initial requirement to simulate three-dimensional VANETs is being in possession of the underlying 3D road network in the first place. Most traffic simulators should already

[1] http://veins.car2x.org/

support the statement of a z-coordinate for the description of nodes (i.e. junctions) and edges (i.e. roads). For SUMO [14], which is used in Veins, this is the case as well. Thus, the actual task is to obtain and import corresponding elevation data.

A straightforward option is the manual definition of nodes and edges including the respective z-coordinate, which can be done using XML. SUMO's network creation tool *netconvert* allows to merge the given data into a normal road network file, which can then be used for simulation. While this approach might be helpful for small artificial scenarios such as a parking garage, it is not reasonable when investigating larger road networks based on real-world maps. In such a case an automated approach using real-world data is desirable.

The solution to this issue are so-called Digital Elevation Models (DEMs). Generally speaking, a DEM can be seen as a collection of height values for a certain set of locations. Most of the data is acquired from radar or laser measurements, either airborne or satellite based. Horizontal resolutions vary from 1 m in highly detailed models to 90 m in coarser data structures. Due to the lack of standardized definitions, there are various terms referring to different kinds of altitude data. However, most experts mainly distinguish two types of DEMs depending on the represented surface as shown in Figure 2 [15], [16]. Digital Surface Models (DSMs) refer to the top-most layer of the Earth's surface. Thus, buildings and vegetation are included in these datasets. On the contrary, Digital Terrain Models (DTMs) represent the real surface of the Earth. It is important to know these differences as the choice of DEM type can affect the generated 3D road network. For example, if a DSM is used to generate the 3D road network, elevated roads such as overpasses and bridges will be assigned wrong altitude values as the dataset only contains the data of the bottom-most surface.

Possible sources for DEMs on the one hand include publicly available datasets as generated by the Shuttle Radar Topography Mission (SRTM) [17] for example. It provides nearly global coverage at a horizontal resolution of about 30 m. Another source for elevation data are public authorities. Most of them offer highly detailed geographic datasets of their region of responsibility, however, this level of detail is usually not freely available any more.

As soon as a suitable DEM has been chosen, it has to be imported into the road network. In case of SUMO, the *netconvert* tool allows the import of elevation data in the form of so-called Shapefiles as well as GeoTIFF files. With the help of the tools provided by the Geospatial Data Abstraction Library (GDAL)[2] it is easily possible to transform the given dataset to the format required by *netconvert*. This way, a given two-dimensional road network can finally be enriched with elevation data.

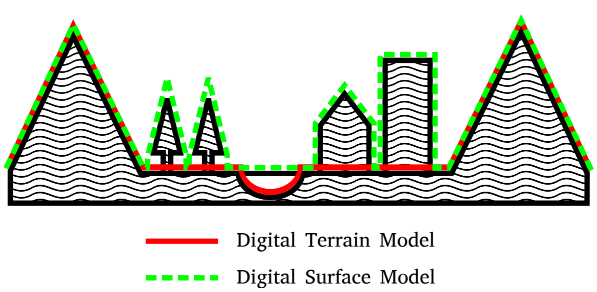

Figure 2. Illustration of the difference between Digital Surface Models (DSMs) and Digital Terrain Models (DTMs).

B. Extensions Towards 3D Network Simulation

After enabling 3D traffic simulation, the network simulator has to properly deal with the additional height information. In case of the Veins framework the mobility simulator SUMO and the network simulator OMNeT++ [18] are coupled via the Traffic Control Interface (TraCI). The first step is to adjust this module so that every vehicle's z-coordinate as well as the slope of the road beneath (and thus the inclination angle of the vehicle) are transmitted along with the remaining parameters. Together with user-provided values for antenna height and offset the actual antenna position in the three-dimensional space can be determined, which is crucial for all further considerations of the wireless transmission.

1) Three-Dimensional Antenna Patterns: We have already mentioned the possibility of assigning 2D antenna patterns [12] when summarizing related work. It is quite obvious that the investigation of three-dimensional environments should instead include consideration of the whole, 3D antenna patterns. In our 2D implementation the user had to state the horizontal (azimuth) pattern of the antenna by defining equidistant samples. Our 3D approach proposed here requires the user to provide one more set of samples, i.e. the vertical (elevation) pattern of the antenna to be modeled.

During the simulation the antenna gains for transmit and receive antenna are then evaluated for each connection. To do so, the azimuth angle ϕ and elevation angle θ of the signal path relative to the vehicle in question have to be determined based on the LOS vector $\vec{v}_{\text{LOS}}$ between sender and receiver and the orientation vector $\vec{v}_{\text{orient}}$ as illustrated in Figure 3. The azimuth angle is calculated using the scalar product:

$$\phi = \arccos\left(\frac{\vec{v}_{\text{orient}} \circ \vec{v}_{\text{LOS}}}{|\vec{v}_{\text{orient}}| \cdot |\vec{v}_{\text{LOS}}|}\right) \quad (1)$$

For the elevation angle the LOS's elevation angle as well as the orientation's elevation angle have to be computed first. The necessary calculations are given as follows:

$$\left.\begin{aligned} \theta_{\text{LOS}} &= \arcsin\left(\frac{v^z_{\text{LOS}}}{|\vec{v}_{\text{LOS}}|}\right) \\ \theta_{\text{orient}} &= \arcsin\left(\frac{v^z_{\text{orient}}}{|\vec{v}_{\text{orient}}|}\right) \end{aligned}\right\} \Rightarrow \theta = \theta_{\text{LOS}} - \theta_{\text{orient}}. \quad (2)$$

After determining ϕ and θ, the antenna gain can eventually be computed. As the simulation has knowledge about the two principal planes only, the antenna gain in the respective direction needs to be interpolated accordingly. In our implementation we used a method originally presented in [19],

[2]http://www.gdal.org/

ISBN 978-3-903176-02-7 © 2018 IFIP

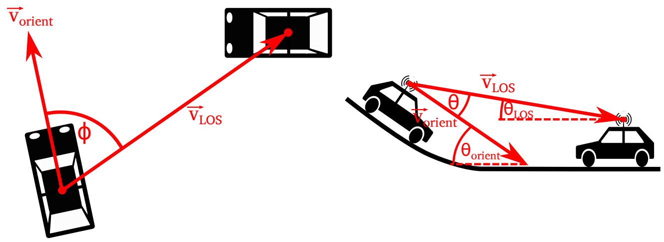

(a) Top-down view (b) Side view

Figure 3. Relevant vectors and angles to determine the 3D signal direction.

which we adjusted and embedded accordingly. It is based on a weighted summing method [20]. The horizontal plane pattern is referred to by $G_\text{H}(\phi)$ and the vertical pattern by $G_\text{V}(\theta)$, where an elevation angle of $\theta = 0$ refers to the horizontal plane. The four closest points for a given direction are then

$$
\begin{aligned}
G_{\theta_1}(\phi) &= \begin{cases} G_\text{V}(\theta = \frac{\pi}{2}) & \text{if } \theta \geq 0, \\ G_\text{V}(\theta = -\frac{\pi}{2}) & \text{if } \theta < 0, \end{cases} \\
G_{\theta_2}(\phi) &= G_\text{H}(\phi, \theta = 0), \\
G_{\phi_1}(\theta) &= G_\text{V}(\phi = 0, \theta), \\
G_{\phi_2}(\theta) &= G_\text{V}(\phi = \pi, \theta).
\end{aligned} \tag{3}
$$

Based on these four gains a horizontal $\hat{G}_\text{Hi}(\phi, \theta)$ and a vertical interpolation value $\hat{G}_\text{Vi}(\phi, \theta)$ are determined:

$$
\begin{aligned}
\hat{G}_\text{Hi}(\phi, \theta) &= G_{\theta_1}(\phi) \cdot W_1(\theta) + G_{\theta_2}(\phi) \cdot (1 - W_1(\theta)), \\
\hat{G}_\text{Vi}(\phi, \theta) &= G_{\phi_1}(\theta) \cdot W_2(\phi) + G_{\phi_2}(\theta) \cdot (1 - W_2(\phi)),
\end{aligned} \tag{4}
$$

where $W_1(\phi)$ and $W_2(\phi)$ are weight functions defined as

$$
W_1(\theta) = \frac{2 \cdot |\theta|}{\pi}, W_2(\phi) = 1 - \frac{|\phi|}{\pi}. \tag{5}
$$

Finally, these horizontal and vertical estimation values are combined with the help of another weight function as follows:

$$
\begin{aligned}
\hat{G}(\phi, \theta) =& \hat{G}_\text{Hi}(\phi, \theta) \cdot W_3(\phi, \theta) + \hat{G}_\text{Vi}(\phi, \theta) \cdot (1 - W_3(\phi, \theta)), \\
W_3(\phi, \theta) =& \frac{2}{\pi} \cdot \left| \left[\frac{\pi}{4} - \left(\frac{\pi}{2} - |\theta| \right) + \frac{\pi}{2} - \left| \left(\frac{\pi}{2} - |\phi| \right) \right| \right] \right|.
\end{aligned} \tag{6}
$$

This yields the final three-dimensional antenna gain value $\hat{G}(\phi, \theta)$, which is subsequently applied on the signal power.

2) Modeling Environmental Diffraction: In case of the conventional 2D approach, the influence of obstacles disturbing communication has not been considered so far as everything appears to be planar (except for the obstacle shadowing model dealing with buildings mentioned before). For 3D VANET simulation this assumption does no longer apply and further sources of attenuation have to be considered, which can be summarized under the term of signal diffraction.

In general, diffraction can be observed whenever waves encounter obstacles, causing bending and deflection of the waves also in theoretically shaded areas. A common way of analyzing diffraction effects is the approximation of obstacles as knife-edges. This method is applicable as long as the obstacles in question are significantly larger than the utilized wavelength, which is the case for IEEE 802.11p based communication in the 5.9 GHz band. Besides the dependence on the wavelength, the geometrical constellation is determined by the distances to sender and receiver d_1 and d_2 as well as the height of the obstacle's top above the LOS h, which is commonly merged into the dimensionless parameter ν [21]:

$$
\nu = h \cdot \sqrt{\frac{2}{\lambda} \cdot \left(\frac{1}{d_1} + \frac{1}{d_2} \right)}. \tag{7}
$$

Referring to the Huygens-Fresnel principle, the attenuation due to diffraction can then be calculated with the help of the Fresnel integrals or the following approximation [21], [22]

$$
J(\nu) = 6.9 + 20 \log \left(\sqrt{(\nu - 0.1)^2 + 1} + \nu - 0.1 \right), \tag{8}
$$

yielding the attenuation in units of dB for $\nu > -0.78$.

As already outlined in Section II, Boban et al. emphasized the impact of other vehicles blocking the signal path [7]. They proposed a method to represent this aspect in simulation using a similar approach based on a multiple knife-edge model. However, the consideration of other vehicles as potential obstacles only is still not sufficient. Another reason for additional signal attenuation is the shape of the surrounding terrain, which can lead to similar effects. One may simply think of a hill between two roads or a road of hilly shape impacting the direct signal path. If a 3D environment is to be considered, this aspect must not be neglected as well. Therefore, we combined both aspects, i.e. diffraction by other vehicles and due to terrain characteristics into an environmental diffraction model.

The main idea is to analyze the LOS and generate a set of knife-edges. We first create a height profile along the signal path. For this purpose, the DEM used for the creation of the 3D road network is queried equidistantly (the interval is adjustable). The obtained height values are added to the set of knife-edges along with their respective distances to the sender. Next, it is necessary to check whether other vehicles are located along the LOS. To do so, the vehicles' bounding boxes are determined. This results in four segments for each vehicle, which are subsequently checked for intersections with the line of sight. If there is an intersection, the vehicle's height (plus its z-coordinate) is added to the set of knife-edges together with its distance to the transmitting vehicle. An illustration of this principle is presented in Figure 4.

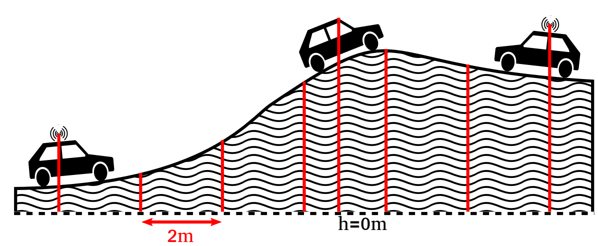

Figure 4. Generation of a set of knife-edges for terrain shape and intermediate vehicles. In this example the terrain point spacing is 2 m (not drawn to scale).

ISBN 978-3-903176-02-7 © 2018 IFIP

Finally, the obtained list of knife-edges is used to approximate the attenuation with the help of the cascaded knife-edge method recommended in ITU Recommendation ITU-R P.526-11 [21]. This approach is in fact a variation of the Deygout method [23] including empirical correction terms. It is based on finding the knife-edges with the highest values for the diffraction parameter ν. For the n-th profile point we get

$$\nu_\text{n} = h \cdot \sqrt{\frac{2 \cdot d_\text{ab}}{\lambda \cdot d_\text{an} \cdot d_\text{nb}}}. \tag{9}$$

Here, d_xy states the distance between the named points, where the indices a and b correspond to sender and receiver. The height above the LOS h is given by

$$h = h_\text{n} + \frac{d_\text{an} \cdot d_\text{nb}}{2 \cdot r_\text{e}} - \frac{h_\text{a} \cdot d_\text{nb} + h_\text{b} \cdot d_\text{an}}{d_\text{ab}}, \tag{10}$$

where h_x refers to the height of the indexed knife-edge. As this method takes into account Earth curvature as well, the effective Earth radius r_e has to be provided as well. It is usually set to $\frac{4}{3} \cdot r_\text{geo} = 8495\,\text{km}$.

The diffraction loss is then determined in three steps.

1) For every knife-edge in the generated list the value for ν has to be computed. The profile point with the maximum value of ν_p is identified as the principal edge. If $\nu_\text{p} > -0.78$ continue with step 2, otherwise 0 dB is returned.
2) Repeat this procedure with the knife-edges between transmitter and principal edge only, which yields ν_t.
3) Repeat this once more with the knife-edges between principal edge and receiver and denote this value as ν_r.

The overall attenuation in dB is finally given by

$$L_\text{diff} = J(\nu_\text{p}) + T \cdot (J(\nu_\text{t}) + J(\nu_\text{r}) + C), \tag{11}$$

where C is an empirical factor defined as $C = 10.0 + 0.04 \cdot D$ with D being the total path length in km. The factor T equals

$$T = 1.0 - \exp\left(-\frac{J(\nu_\text{p})}{6.0}\right). \tag{12}$$

This way the diffraction effects in a three-dimensional VANET environment can be represented and applied on the signal.

IV. Implications on a City-Wide Simulation Scenario

With the help of the outlined extensions it is possible to simulate the impact of a three-dimensional environment on vehicular networks. In this paper, we take a look at two simulation scenarios with a different focus, starting with a city-wide simulation scenario in this section. The general simulation parameters valid for both investigations are summarized in Table I. In order to be able to assign realistic antenna characteristics, we sampled the patterns given in [9], [11], whose azimuth and elevation planes are presented in Figure 5.

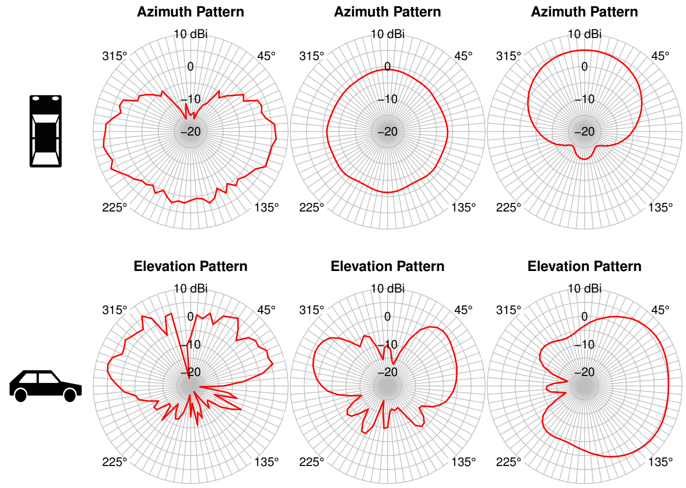

(a) Monopole antenna on panorama glass roof (based on [11])

(b) Monopole antenna (based on [9])

(c) Patch antenna (based on [9])

Figure 5. Azimuth and elevation planes of antenna patterns assigned to simulated vehicles. The gain is given in dBi.

A. Simulation Setup

For our city-wide investigation we made use of the Luxembourg SUMO Traffic (LuST) scenario [24]. It models realistic traffic conditions for a duration of 24 hours in the city of Luxembourg. All vehicles were enabled to send Basic Safety Messages (BSMs) (i.e. beacons) at a frequency of 0.1 Hz. To get an idea of the general implications of a 3D environment, we measured the ratio of received beacons to sent beacons. In simple terms, this ratio states how many neighboring vehicles are in reach and could receive a beacon on average, giving a good overview of the communication conditions.

The three-dimensional antenna patterns shown in Figure 5 were assigned randomly to the vehicles. As the road network used in the LuST scenario is two-dimensional, we had to add elevation data. For this purpose we used a DTM offered by the Austrian OpenDataPortal[3]. It is based on data obtained by airborne laser scans and exhibits a horizontal resolution of 20 m at a vertical resolution of 0.1 m. For the height profile

[3] http://data.opendataportal.at/dataset/dtm-luxembourg

Table I
General Simulation Parameters

Parameter	Value
Penetration rate	100 %
Path loss models	free-space path loss, obstacle shadowing, environmental diffraction
Maximum transmission range	2600 m
Technology	IEEE WAVE
Maximum transmit power	20 mW
Sensitivity threshold	−89 dBm
Thermal noise	−110 dBm
Message type	Basic Safety Messages (BSMs)

ISBN 978-3-903176-02-7

generated by the environmental diffraction model a spacing of 10 m was applied.

For comparison reasons we executed the simulation in two additional configurations. On the one hand, the two-dimensional case with 2D antenna patterns was examined. Here, the same antennas were assumed, however, only the azimuth pattern was considered. In the third configuration, we reproduced the original situation before the support for 2D antenna patterns was added to Veins by assigning isotropic antennas to all cars.

Each simulation was run for a simulated duration of one minute. As the number of vehicles and thus traffic density can have severe influence on the resulting vehicular network, we further analyzed differing starting times of 4am, 5am, 6am and 7am. Therefore, it is possible to see how the observed parameter scales for different traffic demands.

B. Evaluation of Simulation Results

Each setup was repeated eight times to increase the statistical representativeness. The resulting ratios for all configurations are depicted in Figure 6. As can be seen, the average number of neighbors in reach increases for later starting times regardless of the setup in use due to the rising number of vehicles on the roads. While there are only about 400 cars driving at 4am, the value goes up to 3100 cars at 7am as time emerges towards rush hour. Therefore, there are also more potential receivers in close proximity to every vehicle, which is why a broadcasted beacon can be received by more cars.

However, the interesting insight is the difference of neighbors in reach regarding the three different environments. At 4am, the original 2D simulation environment leads to almost nine beacon recipients compared to about three in case of the 3D enabled environment. For later starting times, the results are similar in relation, but the differences get even more significant. While the three-dimensional case delivers a value of about eleven neighbors on average at 7am, the 2D environment including sampled antenna patterns already leads to a value of 26. Omitting antenna patterns causes a further increase to 34 recipients per broadcasted beacon, meaning a

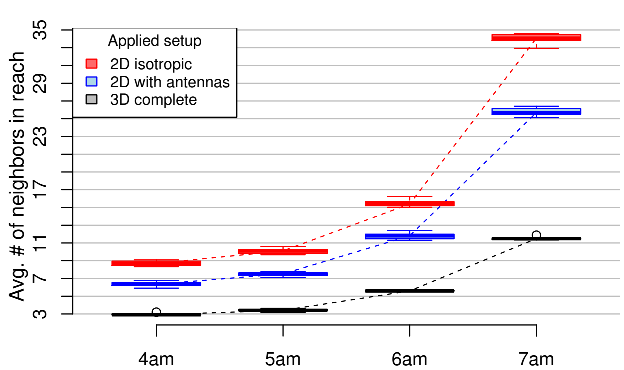

Figure 6. Avg. number of neighbors in reach (i.e. received BSMs/sent BSMs) for different starting times and setups when simulating the LuST scenario.

value about three times as high as the actual three-dimensional count. This enormous difference to the 3D result can be explained with the large number of additional cars diffracting the signal.

Although this simulation scenario and the analyzed metric are rather general, it allows for a first important insight. It is clearly noticeable that the classical two-dimensional approach tends to over-estimate the number of successful packet transmissions. The application of 2D antenna patterns already improved the situation, but it still differs from the three-dimensional case.

V. Impact on a GLOSA System in Steep Environment

While the aim of the first scenario was to get a general impression of the implications of (not) considering a three-dimensional environment, we want to give a deeper insight with the second investigation. Here, we examine how the different approaches influence the functioning of a Green Light Optimal Speed Advisory (GLOSA) system. The basic concept of such an application is to optimally adjust the vehicle's speed when approaching a traffic light based on the knowledge of the signal phase [25]. To do so, the traffic light broadcasts information about its phases, which is received and processed by approaching vehicles.

A. Simulation Setup

In this isolated scenario the ego-vehicle approaches a traffic light which is located on the top of a steep part in downtown Seattle. To generate the three-dimensional road network, we used an elevation model offered by the U.S. Geological Survey as part of the National Elevation Dataset[4] with a horizontal resolution of about 3 m. The resulting road network is depicted in Figure 7. The illustration also shows the vehicle's path starting on 1st Avenue (A). It then turns left on Cherry Street (B) and drives all the way up until it reaches 6th Avenue, which is where the GLOSA traffic light is located (C). Thus, the ego-vehicle climbs about 50 m on its way to the target.

The GLOSA traffic light is modeled as a Roadside Unit (RSU) module with isotropic radiation characteristics. It sends beacons at a frequency of 10 Hz in order to be able to examine how the receive power develops as the vehicle approaches the traffic light. For the car the panorama glass roof antenna pattern has been selected (see Figure 5a). The spacing of profile points in the environmental diffraction model was set to 1 m and the obstacle shadowing model was configured for $\beta = 6\,\mathrm{dB}$ and $\gamma = 0.4\,\mathrm{dB/m}$. Furthermore, 15 other cars were included to drive in front of the ego-vehicle. Finally, we captured the receive power at the ego-vehicle as well as the impact of each attenuation component.

B. Evaluation of Simulation Results

We repeated the simulation for a 2D environment with and without an assigned antenna pattern similar to the first scenario. Figure 8 shows the corresponding results as well as

[4]http://ned.usgs.gov

ISBN 978-3-903176-02-7 © 2018 IFIP

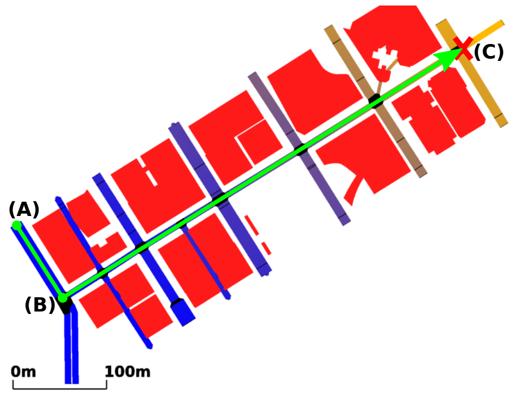

Figure 7. SUMO screenshot showing a 3D road network of downtown Seattle (blue ≙ 10 m, orange ≙ 65 m, red cross ≙ GLOSA traffic light). The car starts on 1st Avenue at (A), turns on Cherry Street at (B) and continues on to (C).

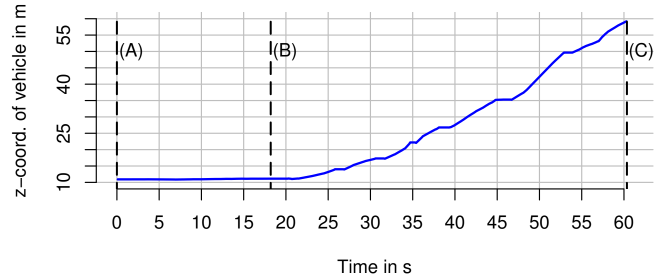

(a) course of the z-coordinate of the ego-vehicle

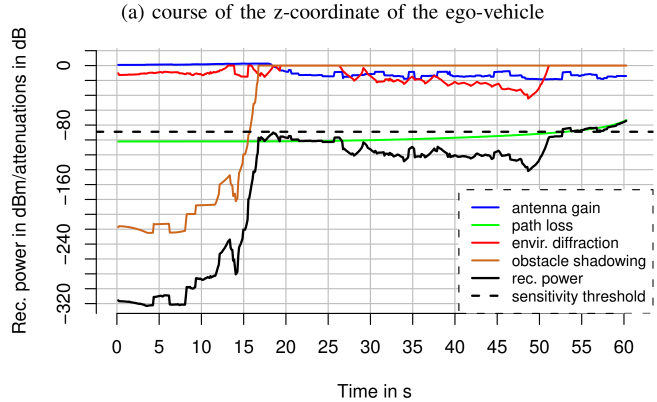

(b) based on 3D environment

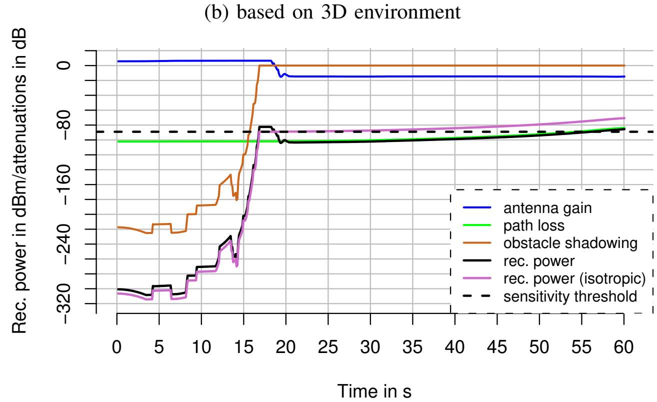

(c) based on 2D environment (antenna pattern/isotropic)

Figure 8. Receive power and attenuation sources for the GLOSA scenario.

the course of the ego-vehicle's z-coordinate. It can be seen that the obstacle shadowing model leads to critical attenuation until a travel time of about 17 s in all three configurations. Obviously, this is caused by buildings blocking the LOS until the car turns left on the final street. Shortly after, the antenna gain (if considered) gets negative as the signal is now received from an azimuth angle of about 0°, which is where the assigned pattern exhibits a significant minimum. Henceforth, the antenna gain fluctuates in case of the 3D simulation as the signal is received from varying elevation angles. In case of the 2D-only environment the antenna gain stays at a constant level as the only angle to be considered is the azimuth angle, which does not change after the car has turned.

As can be seen in Figure 8b, environmental diffraction leads to significant attenuation of up to 40 dB. The fluctuating shape of its curve is caused by two aspects. First, the spatial distribution of the cars driving in front of the ego-vehicle changes continuously. Secondly, the shape of the road towards the target plays an important role. As illustrated in Figure 8a, there are several noticeable steps wherever a junction is located. Thus, diffraction of the signal occurs at the edges of these steps, leading to even higher attenuations.

As a result, the receive power stays below the sensitivity threshold until seven seconds before reaching the target, so that no GLOSA packets can be received until this point. This is certainly not enough time to effectively make use of the main idea of GLOSA systems. Looking at the 2D results, one can notice that the receive power is far less impacted. Applying 2D antenna patterns, the receive power stays below the threshold until a few seconds before reaching the target as well, yet it is quite close to the threshold. However, the neclegtion of antenna patterns (i.e. assuming isotropic antennas) causes the receive power to exceed the threshold after about 17 s. As a consequence, the outcome of the conventional simulation approach without antenna and 3D considerations states that the GLOSA packets would be received in due time, which is clearly wrong when analyzing the more realistic three-dimensional results. In summary, it can be said that disregarding 3D aspects can quickly lead to wrong conclusions due to overoptimistic results.

VI. Conclusion and Future Work

In this paper we have investigated the implications of three-dimensional considerations on vehicular network simulations. Many real-world traffic situations cannot be analyzed reliably based on 2D projections, and yet, this is state-of-the-art in most VANET simulation frameworks. This issue can lead to critical misrepresentations. Thus, we outlined the necessary steps that have to be considered in order to facilitate the simulation of three-dimensional scenarios. On the part of traffic simulation, digital elevation models can be used to generate 3D road networks. On the other hand, we incorporated models to deal with three-dimensional antenna patterns as well as diffraction effects caused by the terrain shape and cars along the LOS.

ISBN 978-3-903176-02-7

Finally, we demonstrated the impact of the 3D extensions by simulating two selected scenarios. The first investigation based on analyzing the average number of neighboring vehicles in reach in a city-wide scenario showed that 2D-only simulations constantly overestimate the neighbors count. Secondly, we analyzed a more specific case with a fictional GLOSA setup. It could be seen that the influence of antenna patterns and diffraction effects causes significant additional attenuation. Thus, the proper operation of a GLOSA system based on a three-dimensional investigation would be questionable, while the original simulation approach would not attest any problems.

Although the focus of this paper was on the actual simulation results, we would also like to mention that the presented 3D extensions can lead to increased simulation durations. The city-wide 7am simulation originally ran more than four days (compared to about three hours in case of the 2D approach). This is mainly caused by the environmental diffraction model, which requires the analysis of the height profile as well as potential cars in the LOS for every possible connection within maximum transmission range. However, we optimized the performance by caching altitude values and excluding cars that cannot be located between sender and receiver by organizing all vehicles in a global grid. This way, the runtime could be decreased to a reasonable value of about eight hours.

In summary it can be concluded that conventional 2D VANET simulation often yields overoptimistic results due to the neglection of many potential sources of signal attenuation. As simulation is a key tool and widely used to develop and evaluate protocols and applications, this shortcoming can lead to wrong conclusions. Therefore, it is necessary to consider three-dimensional aspects as well in order to obtain more valuable and reliable results.

Nonetheless, our proposed extensions are not yet sufficient for the investigation of arbitrary three-dimensional scenarios. Referring to the introductory example scenario, it becomes clear that the impact of floors or ceilings should not be neglected as well. Thus, a model which identifies floors intersecting the LOS and estimates the resulting attenuation is part of future work. Furthermore, it would be desirable to validate the models implemented in the course of this work by conducting field tests and real-world measurements.

References

[1] C. Sommer, J. Härri, F. Hrizi, B. Schünemann, and F. Dressler, "Simulation Tools and Techniques for Vehicular Communications and Applications," in *Vehicular ad hoc Networks - Standards, Solutions, and Research*, C. Campolo, A. Molinaro, and R. Scopigno, Eds., Springer, May 2015, pp. 365–392.

[2] C. Sommer, D. Eckhoff, R. German, and F. Dressler, "A Computationally Inexpensive Empirical Model of IEEE 802.11p Radio Shadowing in Urban Environments," University of Erlangen, Dept. of Computer Science, Technical Report CS-2010-06, Sep. 2010.

[3] D. Eckhoff, C. Sommer, and F. Dressler, "On the Necessity of Accurate IEEE 802.11p Models for IVC Protocol Simulation," in *75th IEEE Vehicular Technology Conference (VTC2012-Spring)*, Yokohama, Japan: IEEE, May 2012, pp. 1–5.

[4] C. Sommer, R. German, and F. Dressler, "Bidirectionally Coupled Network and Road Traffic Simulation for Improved IVC Analysis," *IEEE Transactions on Mobile Computing*, vol. 10, no. 1, pp. 3–15, Jan. 2011.

[5] B. Karp and H. T. Kung, "GPSR: Greedy Perimeter Stateless Routing for Wireless Networks," in *Proceedings of the 6th Annual International Conference on Mobile Computing and Networking*, ser. MobiCom '00, Boston, Massachusetts, USA: ACM, 2000, pp. 243–254.

[6] Q. Lin, C. Li, X. Wang, and L. Zhu, "A Three-Dimensional Scenario Oriented Routing Protocol in Vehicular Ad Hoc Networks," in *2013 IEEE 77th Vehicular Technology Conference (VTC Spring)*, Dresden, Germany: IEEE, 2013, pp. 1–5.

[7] M. Boban, T. Vinhosa, J. Barros, M. Ferreira, and O. K. Tonguz, "Impact of Vehicles as Obstacles in Vehicular Networks," *IEEE Journal on Selected Areas in Communications*, vol. 29, no. 1, pp. 15–28, Jan. 2011.

[8] M. Boban, R. Meireles, J. Barros, P. Steenkiste, and O. K. Tonguz, "TVR – Tall Vehicle Relaying in Vehicular Networks," *IEEE Transactions on Mobile Computing*, vol. 13, no. 5, pp. 1118–1131, 2014.

[9] D. Kornek, M. Schack, E. Slottke, et al., "Effects of Antenna Characteristics and Placements on a Vehicle-to-Vehicle Channel Scenario," in *2010 IEEE International Conference on Communications Workshops*, IEEE, Capetown, South Africa, May 2010, pp. 1–5.

[10] L. Reichardt, T. Fügen, and T. Zwick, "Influence of Antennas Placement on Car to car Communications Channel," *3rd Conference on Antennas and Propagation, EuCAP 2009*, Mar. 2009.

[11] A. Kwoczek, Z. Raida, J. Láčík, et al., "Influence of Car Panorama Glass Roofs on Car2car Communication," in *3rd IEEE Vehicular Networking Conference (VNC 2011), Poster Session*, Amsterdam, Netherlands: IEEE, Nov. 2011, pp. 246–251.

[12] D. Eckhoff, A. Brummer, and C. Sommer, "On the Impact of Antenna Patterns on VANET Simulation," in *8th IEEE Vehicular Networking Conference (VNC 2016)*, Columbus, OH: IEEE, 2016, pp. 17–20.

[13] M. Schiller, A. Knoll, M. Mocker, and T. Eibert, "GPU accelerated ray launching for high-fidelity virtual test drives of VANET applications," in *2015 International Conference on High Performance Computing Simulation (HPCS)*, Amsterdam, Netherlands: IEEE, 2015, pp. 262–268.

[14] D. Krajzewicz, J. Erdmann, M. Behrisch, and L. Bieker, "Recent Development and Applications of SUMO – Simulation of Urban MObility," *International Journal On Advances in Systems and Measurements*, vol. 5, no. 3&4, pp. 128–138, 2012.

[15] C. Hirt, "Digital Terrain Models," in *Encyclopedia of Geodesy*, E. Grafarend, Ed., Cham, Germany: Springer International Publishing, 2014, pp. 1–6.

[16] Z. Li, C. Zhu, and C. Gold, *Digital Terrain Modeling: Principles and Methodology*. CRC Press, 2004.

[17] T. G. Farr, P. A. Rosen, E. Caro, et al., "The Shuttle Radar Topography Mission," *Reviews of Geophysics*, vol. 45, no. 2, 2007.

[18] A. Varga and R. Hornig, "An Overview of the OMNeT++ Simulation Environment," in *Proceedings of the 1st International Conference on Simulation Tools and Techniques for Communications, Networks and Systems & Workshops*, ser. Simutools '08, Marseille, France: ICST, 2008, pp. 1–10.

[19] N. R. Leonor, R. F. S. Caldeirinha, M. G. Sánchez, and T. R. Fernandes, "A Three-Dimensional Directive Antenna Pattern Interpolation Method," *IEEE Antennas and Wireless Propagation Letters*, vol. 15, pp. 881–884, 2016.

[20] F. Gil, A. R. Claro, J. M. Ferreira, C. Pardelinha, and L. M. Correia, "A 3-D extrapolation model for base station antennas' radiation patterns," in *IEEE VTS 50th Vehicular Technology Conference*, vol. 3, Amsterdam, Netherlands: IEEE, 1999, pp. 1341–1345.

[21] ITU, "Recommendation ITU-R P.526-11 – Propagation by diffraction," International Telecommunication Union, Recommendation, 2009.

[22] T. Rappaport, *Wireless Communications: Principles and Practice*, ser. Prentice Hall communications engineering and emerging technologies series. Prentice Hall PTR, 2002.

[23] J. Deygout, "Multiple knife-edge diffraction of microwaves," *IEEE Transactions on Antennas and Propagation*, vol. 14, no. 4, pp. 480–489, 1966.

[24] L. Codeca, R. Frank, and T. Engel, "LuST: a 24-hour Scenario of Luxembourg City for SUMO Traffic Simulations," in *SUMO User Conference 2015 - Intermodal Simulation for Intermodal Transport*, Berlin, Germany, May 2015.

[25] D. Eckhoff, B. Halmos, and R. German, "Potentials and limitations of Green Light Optimal Speed Advisory systems," in *2013 IEEE Vehicular Networking Conference*, Boston, MA: IEEE, 2013, pp. 103–110.

ISBN 978-3-903176-02-7 © 2018 IFIP